Hindawi
Journal of Robotics
Volume 2022, Article ID 7562164, 10 pages
https://doi.org/10.1155/2022/7562164

Research Article

Compliant Mechanism Soft Robot Design and Peristaltic Movement Optimization Using Random Search

L. A. Páramo-Carranza,[1] **A. Lopez-González**,[1] **and Juan C. Tejada**[2]

[1]*Universidad Iberoamericana, Mexico City, Mexico*
[2]*Universidad EIA, Medellín, Colombia*

Correspondence should be addressed to A. Lopez-González; alexandro.lopez@ibero.mx

Received 28 February 2022; Accepted 30 March 2022; Published 12 April 2022

Academic Editor: L. Fortuna

In this article, we use the concept of auxetic structures as inspiration for the design of a compliant mechanism that allows the integration of a soft robot whose movement is based on the peristaltic movements of invertebrates. The TPU mechanism allows for smooth movement of the robot using only two servo motors. To guarantee maximum displacement, a time and angle optimization procedure using photogrammetry and random search was carried out, allowing the advance distance of the soft robot to be maximized.

1. Introduction

One of the objectives of robot design is to imitate human and animal behavior in order to create machines capable of coexisting in our environment and working alongside us [1]. There is also a strong motivation to emulate the softness of human and animal tissue to ensure safe interaction between humans and robots by developing actuators and sensors that allow moving conformable and deformable structures [2, 3]. In robotics, this field of study is called soft robotics and promises the safe interaction between living beings and robots [4] using soft materials, tensegrity [5], bending materials [6], jamming [7], and other technologies.

Soft robots are biologically inspired machines [8] because nature uses softness and compliance in many ways to design biological organisms, which can interact with the environment using body deformations for both object manipulation and locomotion [9]. Venturing into the field of soft robotics requires the development of new soft structures with more natural behaviors, integrated topology with materials, and continuous and conformable bodies. Soft robots have social, biomedical, rehabilitation, exploration applications, and many others [10, 11].

The capabilities of a soft robot are based on its material and the morphology of its structure [12]. Hence, materials and structure are very relevant for the design and manufacture of new mechanisms. The variety of materials used in soft robotics is amazing, where structure, sensor, and soft actuator manufacturing include hydrogels, ionic and conducting polymers, carbon nanotubes, dielectric elastomers, shape-memory materials, and so on [10, 13].

1.1. Metamaterials and Auxetic Materials. Metamaterials are artificial compounds that exhibit, by their structure, properties not available in natural materials. Mechanical metamaterials are designed with specific internal structural elements that allow special and advantageous behaviors over conventional materials. Specific geometric pattern structures provide metamaterials with desirable properties. For example, honeycomb cell design generates interesting negative Poisson's ratio behaviors [14].

A material with a negative Poisson's ratio is called auxetic metamaterial. The word auxetic comes from the Greek "auxetikos" which means "that which tends to grow." Poisson's ratio of a material (ν) tells us how much a material

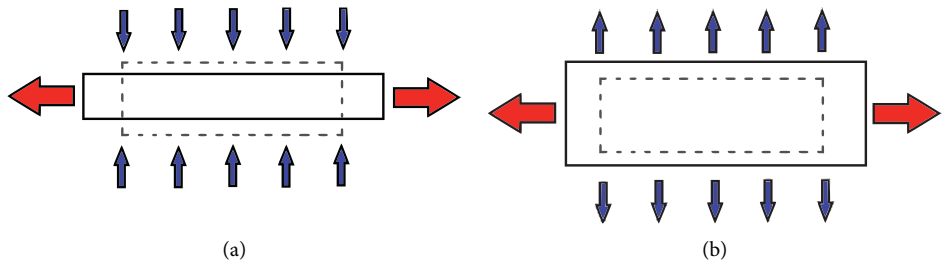

(a) (b)

Figure 1: The original material depicted in dashed lines is subjected to the longitudinal strain represented by the red arrows. (a) Nonauxetic behavior where the original material contracts in the direction of the blue arrows, while (b) an auxetic behavior where the original material expands in the direction of the blue arrows.

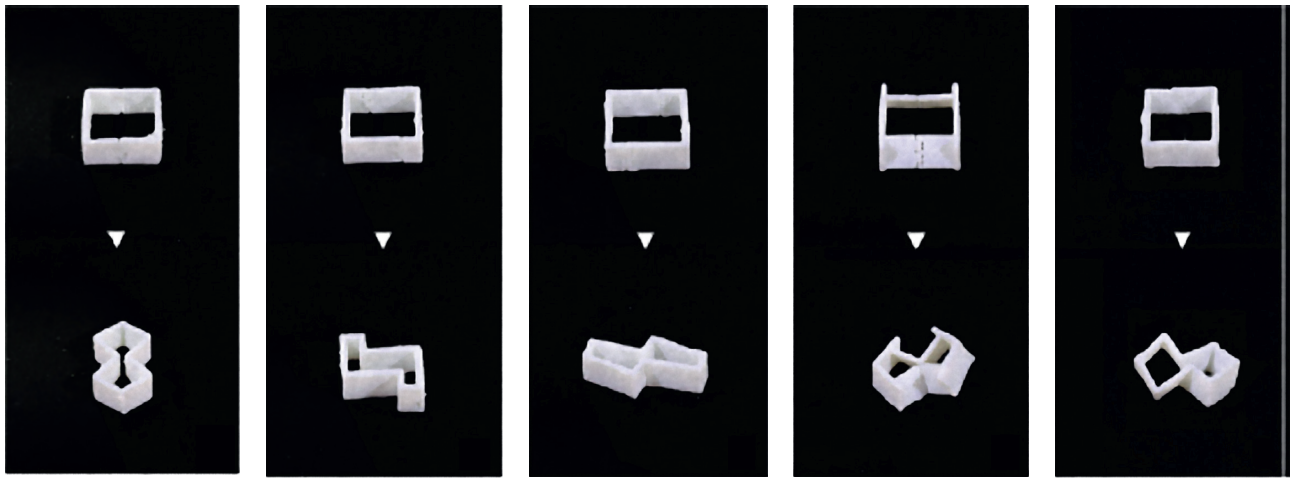

(a) (b) (c) (d) (e)

Figure 2: Auxetic modules developed in [22].

becomes thinner when it is stretched, formally it is defined as the ratio of the lateral contractile strain to the longitudinal tensile strain for a material undergoing tension in the longitudinal direction. Most materials exhibit a positive ν, but auxetic materials have a negative Poisson's ratio. That is, auxetic materials undergo lateral expansion when stretched longitudinally and become thinner when compressed [15, 16], as shown in Figure 1, then:

$$\nu = -\frac{\varepsilon_{\text{trans}}}{\varepsilon_{\text{long}}}, \tag{1}$$

where $\varepsilon_{\text{trans}}$ is the transverse strain, and $\varepsilon_{\text{long}}$ is the longitudinal strain [17]. As mentioned in [18], Poisson's ratio for a stable material is limited between −1 and +0.5 for three-dimensional structures and between −1 and 1 for two-dimensional structures.

1.2. Previous Work. Many articles have been published on the design of actuators based on the principles of auxetic mechanisms [19], conventional robot structural elements [14], as well as soft robots and structures [20–23]. Researchers have been exploring metamaterials that exhibit auxeticity and their applications [24–26].

In [27], the authors use an auxetic mechanism based on a two-dimensional arrangement involving rigid squares connected to each other at their vertices by hinges, achieving a negative Poisson's ratio. These geometric structures are extremely useful and important as they can help researchers better understand how auxetic effects can be achieved and how auxetic materials can be manufactured, as well as how their properties can be optimized and predicted.

In [22], five structures have been developed based on the auxetic configurations of rotating squares. The structure known as KinetiX presents a novel set of cells that can be arranged in such a way that generates different types of movements. This type of cell is a square structure to which hinges are placed in different positions of each bar, always maintaining symmetry in between parallel bars, as shown in Figure 2. Hence, a contraction or expansion of the bars generates the desired deformation allowing uniform scaling, shear, bending, and rotation.

Jifei Ou and his colleagues [22] built on the structures presented by Evans [15] and Saxena [28], rotating square structures to generate a four-bar mechanism shown in Figure 3. It is based on four rectangles joined at one of their vertices. These joints $(h_0, \ldots, h_3)$ are used as hinges and compose a two-dimensional movement.

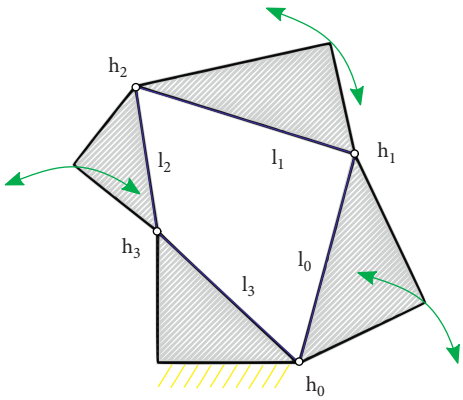

Figure 3: Four bar mechanism.

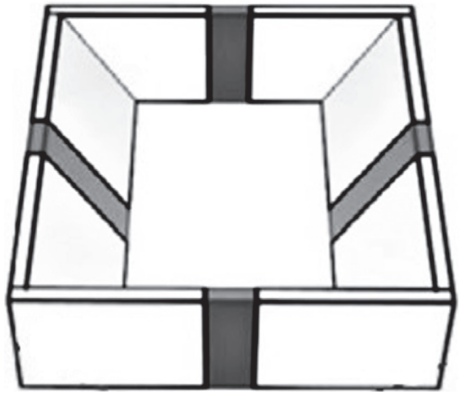

Figure 4: Bending configuration cell [22].

Using the Chebychev–Grübler–Kutzbach criterion [29, 30], as shown in equation (2), where the number of rigid bodies is $N = 4$, the number of joints $j = 4$, and joints with only have one degree of freedom $f_0, \ldots, f_3 = 1$, the four-bar mechanism in Figure 3 has only one degree of freedom.

$$M = 3(N - 1 - j) + \sum_{n=1}^{j} f_n. \quad (2)$$

Two types of three-dimensional transformations were developed: hinge-in plane rotation and hinge-out plane rotation, both described in [22], and five single units of planar and spatial transformation are shown in Figure 2.

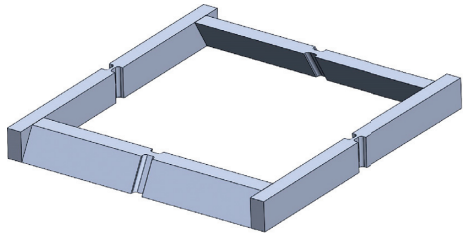

Figure 5: Auxetic cell design.

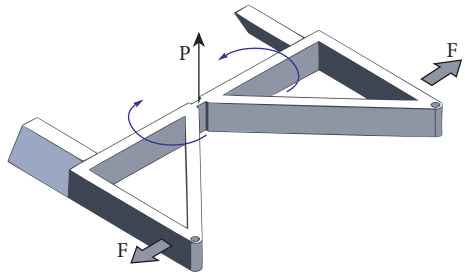

Figure 6: Reinforced section, the force is applied to the corners.

However, the one that inspired the present work is hinge-out plane rotation (bending spatial transformation), where the four hinges are angled at $(\pi/2)$ on the plane of rotation and located in the middle of each bar. Each wall is given an inclination angle β, as shown in Figure 4. This combination of angles creates a rotation out of the hinge's plane. The design of this structure is such that when a tensile force is applied, a bidirectional expansion is generated.

2. Auxetic-Inspired Bending Structure

We developed a soft material structure capable of bending out of its geometric plane from a single degree of freedom. These characteristics allow the mechanism to be used as a link in a soft robot. We use this mechanism to provide locomotion to a bipedal robot using peristaltic movements with a single degree of freedom for each leg. This type of mechanisms allows to simplify the redundance diffculties of use a cable-driven actuation [31, 32]. The structure, shown in Figure 5, is based around a 50 mm square cell.

By placing a triangular structure at each end of the mechanism, we are allowing the force necessary to bend the mechanism to be applied at each point of the protruding triangle. It was observed that these links, which are made of soft material, did not manage to transmit movement. This is why a reinforcement was placed, joining the section with a bar of the same dimensions as the designed mechanism. The movement is generated by applying force in the corners, keeping the central hinge, point P, as the axis of rotation, as depicted in Figure 6.

2.1. Compliant Hinges. To manufacture the structure using only soft material, the use of bolts and rotation axes was avoided by replacing the hinges from the original mechanisms with compliant hinges. A structural part of a compliant mechanism can be seen as a compliant joint. If two

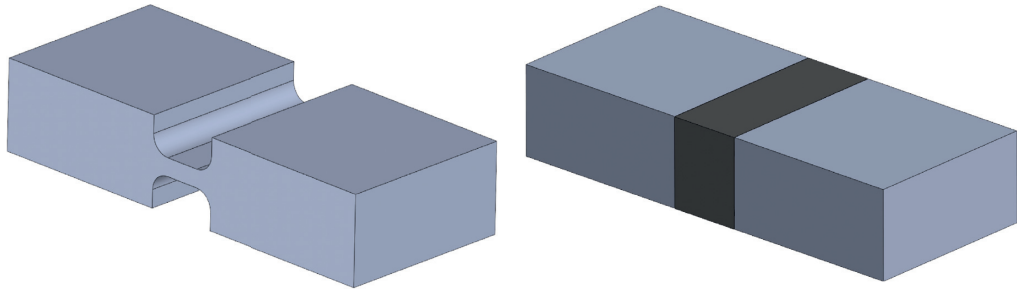

(a) (b)

Figure 7: Two different compliant joints with relative motion.

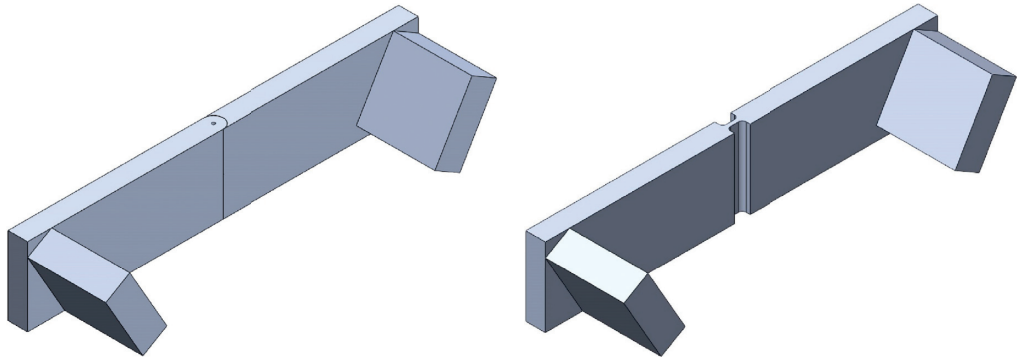

(a) (b)

Figure 8: Original hinge (a) and compliant hinge (b).

links are coherently united, then it is known as a compliant coherent joint. This allows at least one relative motion between links, but it is often limited to a localized area [33, 34]. Such union in a compliant mechanism is achieved in two ways, as depicted in Figure 7, changing the material and changing the geometry in the area where different stiffness is required.

To manufacture the mechanism in a single piece and completely from soft material, the flexible hinges were made by changing the geometry of the bars and placing them at the middle point of each link to obtain a symmetrical flexion, as shown in Figure 8.

With this, the mechanism inherits the properties and advantages that compliant hinges have against classic hinges [33, 34]; a smaller one-piece, one-material design, no rigid materials, axes, or fasteners, and needless lubrication since there is no friction between parts.

2.2. 3D Printed Mechanism. A thermoplastic polyurethane (TPU) was used to print the mechanism, as shown in Figure 9. For the structure to function as a soft robot actuator and locomotion mechanism, the application of a force on the two corners of the mechanism is needed, which cause a rotation with regard to the axis P. A gripper-like mechanism was designed with polylactic acid (PLA) gears, as shown in Figure 10, actuated by a servo motor as Sg90 Tower Pro with a maximum torque of 2.5 kg cm and a weight of 14.7 g in order to provide such forces but not add to its weight. This allows opening and closing the triangular supports of the mechanism with a single motor.

2.3. Motion Mechanism. The simple gear transmission consists of a driving wheel with teeth on its outer periphery, which meshes with a similar one, thereby preventing slippage between wheels. The system also reverses the direction of rotation of two contiguous axes, which allows the blades to move in opposite directions for G_1 and G_2, thereby stretching the mechanism. Both of these have a diameter of 24 mm. The gear attached to the motor is a spur gear G_0 with 13 teeth and a base diameter of 12 mm. It is responsible for transmitting the engine torque.

Each gear, G_1 and G_2 have 24 gear teeth and are mechanically engaged with a 1 : 1 ratio. The driving gear attached to the motor has 12 teeth and is in charge of transmitting the movement torque. This gear has contact only with gear G_2, with which it has a transmission ratio of 1 : 2; therefore, the torque increases. The force exerted on the corner of the soft mechanism can be calculated from the gear ratio, considering that the torque delivered by the motor is $\tau_1 = 1.8\text{kg/cm}$ and using the gear transmission ratio, the torque produced in gear two is $\tau_2 = 3.6\text{kg/cm}$.

From this torque, the force exerted on the mechanism can be calculated by taking the stem of the gear as a cantilever beam, with a lever arm of 2 cm, $F = \tau \cdot l = (3.6\,\text{kg/cm}) \cdot (2\,\text{cm}) = 7.2\text{kg}$. Therefore, the applied force at each corner is about 70.63 Newtons.

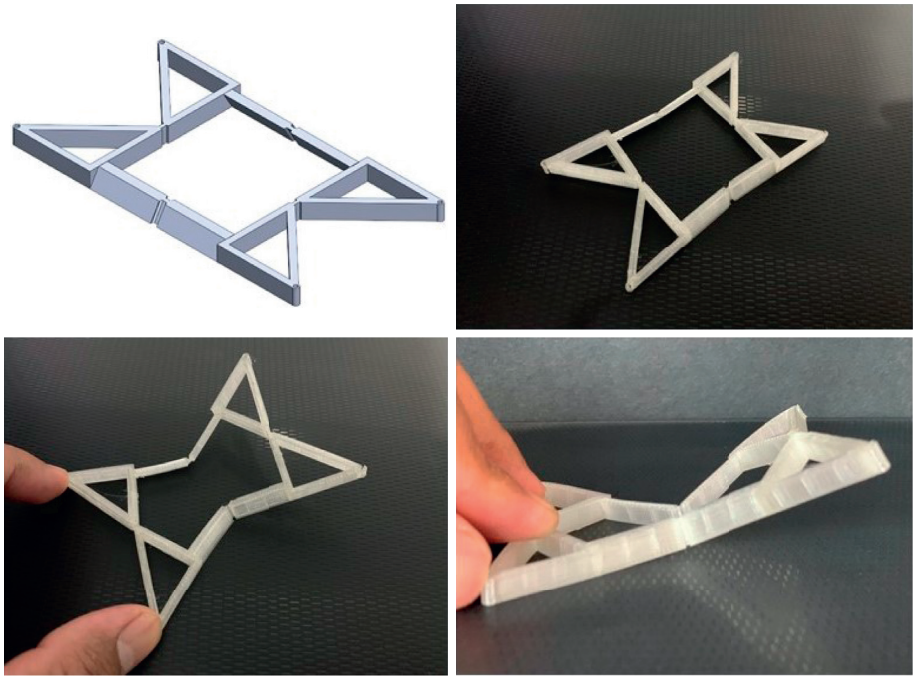

Figure 9: CAD design and mechanism 3D printed in TPU.

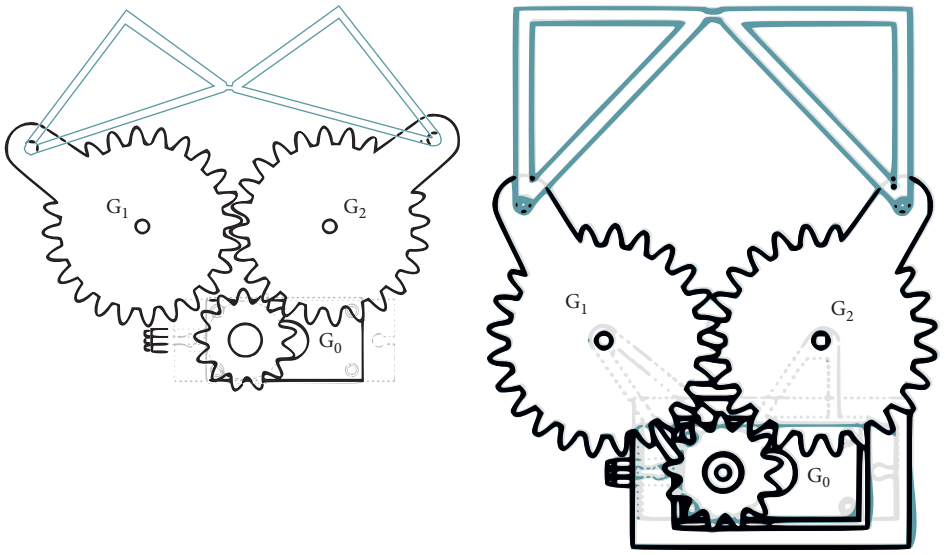

(a) (b)

Figure 10: Movement generated by the gears to bend the mechanism.

The PLA plastic base that supports the gear train is shown in Figure 11. This piece allows the rotation of each gear. It keeps the gears at the appropriate positions for their correct operation. The complete system, assembled with the designed mechanism, is shown in Figure 12.

3. Soft Robot Locomotion and Optimization

This actuation mechanism is used in the construction of a mobile soft robot. It is considered a limb of the bipedal robot since, properly placed, it can generate a push on the surface [35]. The bipedal soft robot is displayed in Figure 13.

The movement of the robot is biologically inspired, specifically from worms, which move from cycles of contractions and relaxations of certain sections of its body that cause them to periodically expand and contract their length. With this type of movement, the robot is capable of advancing in each cycle. This is not properly a worm movement since the same source of locomotion is not applied as it has been developed in many other pieces of research such as

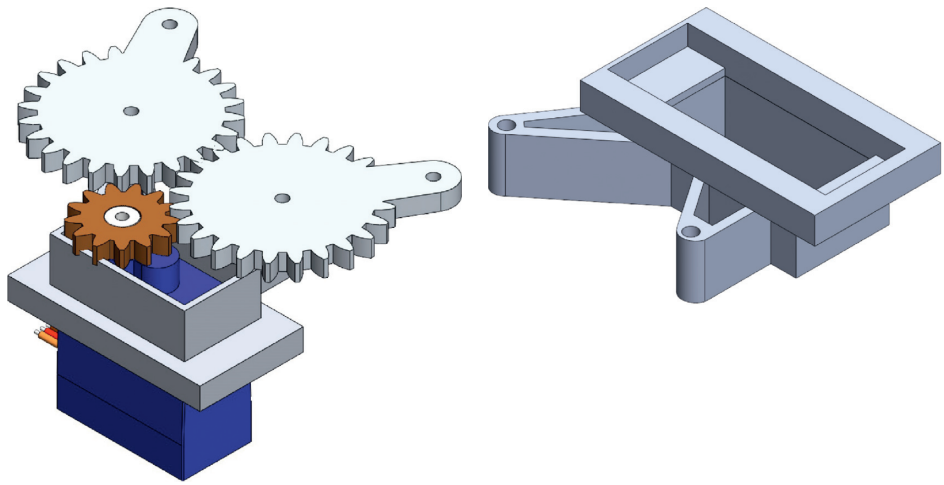

(a) (b)

Figure 11: Gripper-like mechanism.

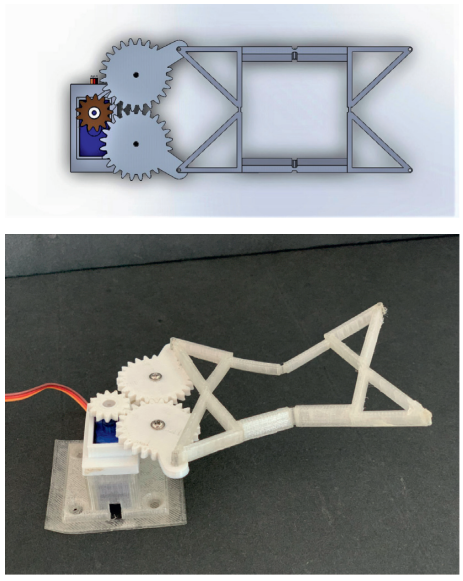

Figure 12: Assembled mechanism.

[9, 36, 37], where the designed robots are themselves robot worms. However, the use of our soft actuator achieves a similar movement.

By having two limbs, it is possible to combine the contraction movements of these links sequentially in a cycle of four steps with a period, to allow the robot to pull and push on the movement plane, thus achieving a displacement. Figure 14 shows how this cycle of contractions and retractions of the links makes the robot advance. At each step, the robot just moves forward a few millimeters.

The distance it travels depends largely on the action sequence of each motor; that is, the independent contraction of each link, the time that each motor waits to return to its initial position, and the maximum actuation. The latter is very important. It is a logical assumption that to achieve maximum displacement, it is necessary to contract the mechanism as much as possible; however, this is not the case.

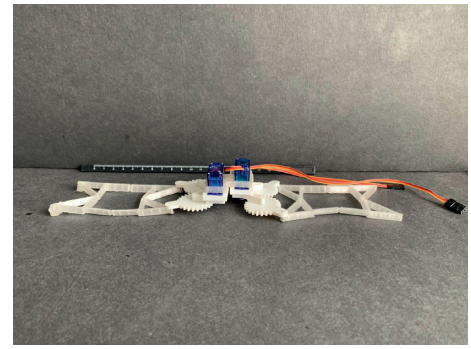

Figure 13: Bipedal soft robot.

It was observed from tests with fixed angles (θ_1 and θ_2) that after the contraction of the link, the link is required to return to its initial position when the servomotor is positioned at zero.

3.1. Random Search Optimization. The movement of soft robots, as well as their control, depends on the mathematical model that describes their dynamics; however, the modeling of soft robots is quite a complicated aspect due to high nonlinearity. Therefore, the application of control methodologies is complicated. This work seeks to maximize the movement of the robot, where analyzing from testing, it was observed that this depended directly on the angles of contraction of the mechanisms and the sequence in which they happen. Later, it was detected that to enhance the movement of the robot, we needed to find the best values of the angles that maximized the displacement. It was necessary to use some optimization techniques; to achieve this, there are many methodologies to find the most suitable parameters that allow maximum displacement, such as genetic algorithms, simulated annealing, hill climbing, random search, random forest, particle swarm optimization, and many others. The random search algorithm was selected to optimize the angle values because it allows us to easily calibrate

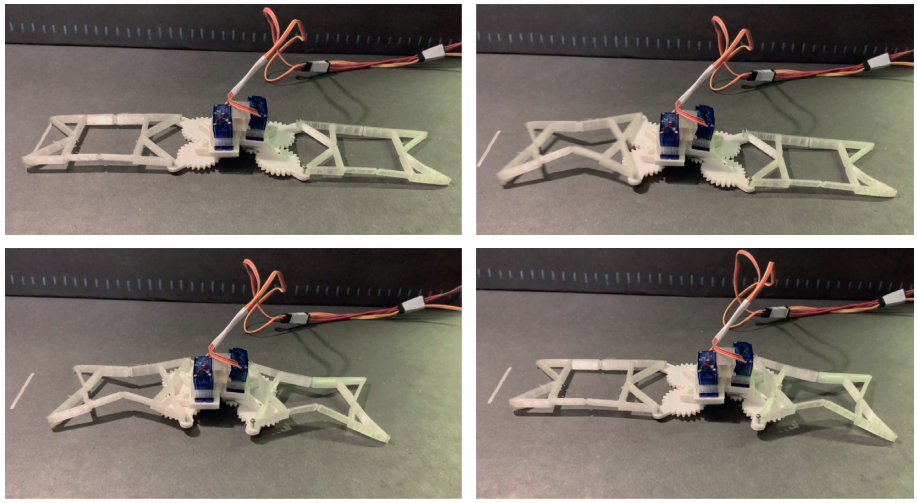

Figure 14: Robot movement: step contractions that generate a displacement of millimeters.

Initialize q in the start point q_i:
while $q \neq q_f$ **do**
  Choose a point $q = [\theta_1, \theta_2, t_1, t_2]$ in the sample space as a starting point;
  Generate a random q_n set and evaluate the performance metric: maximum distance d
  if $d(q_n) > d(q)$ **then**
    $q = q_n$
  else
    search new vector q_n to be analyzed
  end
end

Algorithm 1: Random search.

different robot platform operations [38]. The random search algorithm [39] is presented in Algorithm 1.

The servomotor angles θ_1 and θ_2 are sent employing an Atmega328 microcontroller and t_1 and t_2 are the times that the mechanism remains contracted, then the mechanism returns to its original position.

To know how much the robot has moved, it is necessary to know the new position of the robot in the work area. The photogrammetry procedure is used to measure the robot's displacement by documenting images sequentially through a camera [40]. A green circle was placed on the robot as shown in Figure 15, which is used as the reference position of the robot and is detected in the image through an algorithm written on MATLAB®.

The algorithm begins by taking a capture of the mechanism through the camera by calculating and marking its initial position on the screen with a yellow cross, as shown in Figure 15. In one cycle, the algorithm sends values of position angles to each motor, as well as the time that each motor must wait to return to its initial position. Once the robot has moved, the algorithm calculates the new position of the robot and computes the robot's displacement. Subsequently, it compares the distance traveled with the previous one and decides whether to calculate new random values or to use the same ones. This process continues for one hundred cycles.

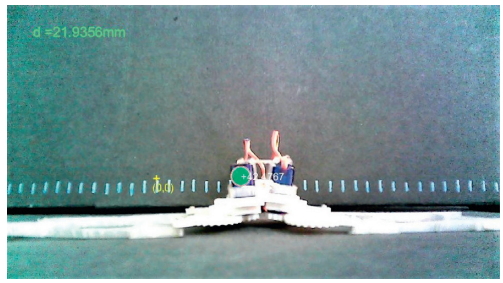

Figure 15: Display of the distance traveled from an initial point.

With the data obtained by the random search optimization, the vector of parameters that achieves the greatest distance traveled is selected and used for a verification stage contrasting performance with fixed maximum angles.

3.2. Optimization Results. The values presented in the following graphs correspond to the vector q in random search. The first graphs are focused on showing the random variation of the angles θ_1, θ_2 that were used in the random search.

The displacement achieved for θ_1, θ_2, t_1, and t_2 through the random search algorithm is considerably greater than that achieved when the fixed angles and waiting times are

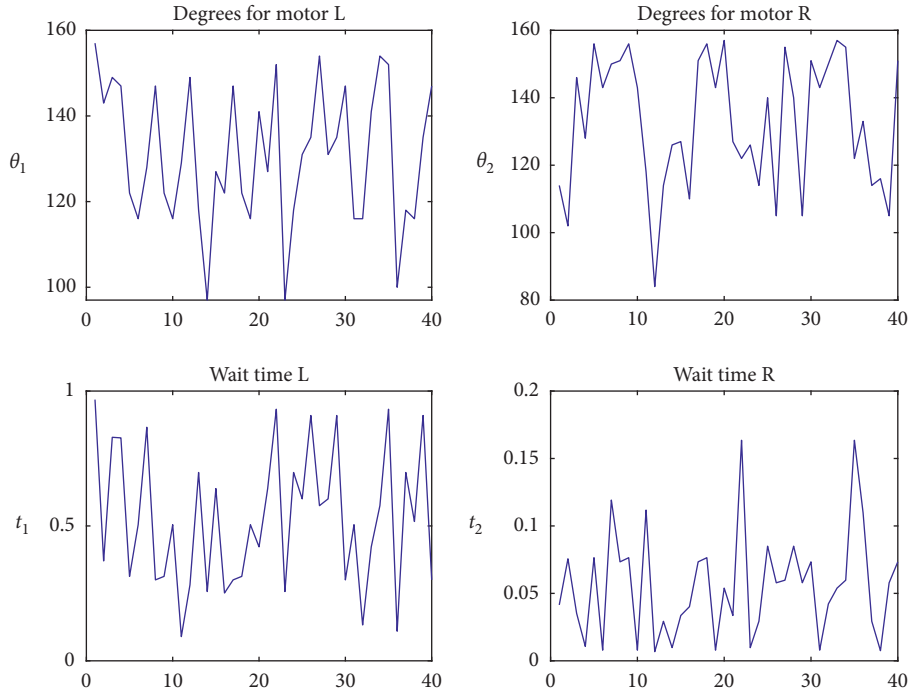

Figure 16: Maximum actuator values for (θ_1, θ_2) and (t_1, t_2).

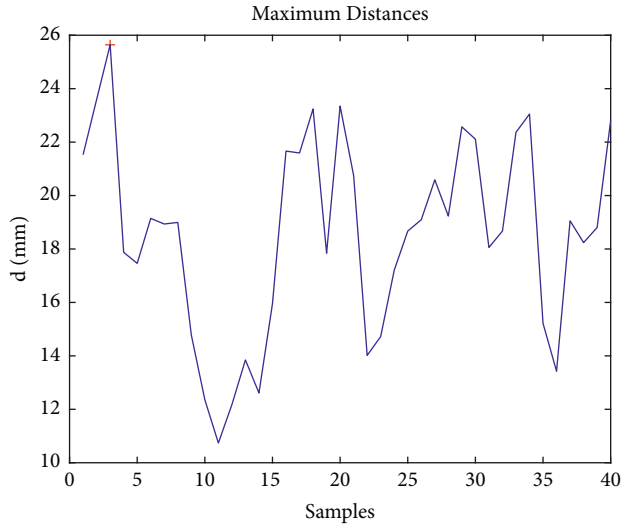

Figure 17: Maximum values of reached distances.

Table 1: Motor angles to generate link shrinkage.

Parameter	θ_1	θ_2
Optimal degrees	149	146
Fixed degrees	160	160

Table 2: Maximum contraction and extension times.

Parameter	Contracted		Extended	
Time	t_1	t_2	t_1	t_2
	0.82	0.03	0.90	0.62

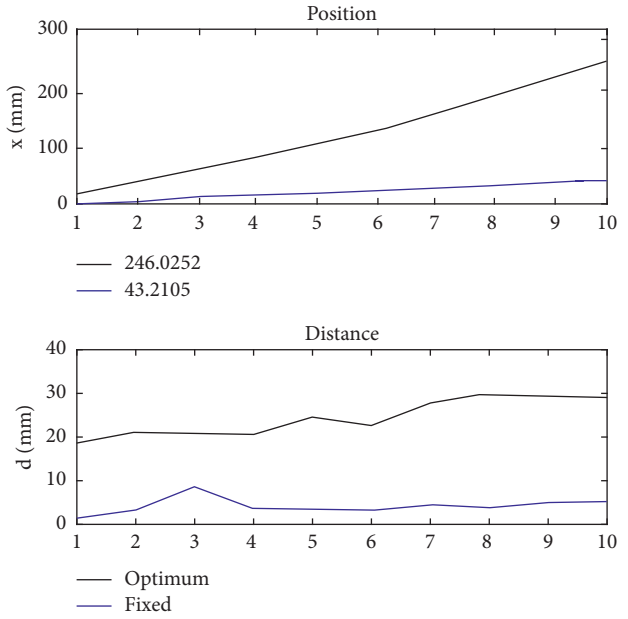

Figure 18: Comparative graph, fixed values (blue) versus optimal parameters (black).

chosen. Figure 16 shows the angle variation and times found by random search throughout fifty iterations of the search cycle.

Since the random search algorithm requires a considerable number of tests to search for the optimal values of angles and times in the robot's movement, 40 search tests for parameters were carried out. Each of these tests consisted of 100 iterations. Once we had all the statistical data of the 40 maximums of each test, the maximum value of this new set

Table 3: Comparison between distance traveled with optimal values and fixed values.

Test	d_{max}	d_{avg}
Optimal values	21.94	21.24
Fixed values	1.4	0.6

was obtained, and the average value of the distances was calculated, as shown in Figure 17.

The maximum distance that the robot traveled from among all cycles was $d = 25.64$ for which the maximum values are depicted in Table 1, which shows the angles at which the motors must move, remembering that they return to the zero initial position at time t. Table 2 displays the contraction and extension times for each motor.

Once the maximum parameters were obtained, they were applied to the robot, and the photogrammetry process was carried out to verify the distances obtained at each step of the robot. The results were compared with those obtained when fixed values are chosen for the parameters of the vector q. The total path was observed during ten iterations or ten steps of the robot in the photogrammetry, also measuring the distance in each step. The graph in Figure 18 exhibits the comparison between both experiments from a starting point as well as the advance distances at each step. Table 3 also shows the values obtained for each of the experiments.

4. Conclusion

A mechanism was developed from a bending cell, redesigning the hinges for a mechanism with coherent, compliant hinges, which made it easier to manufacture into a single piece from flexible TPU material. This compliant mechanism was converted into a soft actuator using gears and a servo motor, using it as legs for a bipedal mobile soft robot.

The movement of the bipedal soft robot was defined by actuator angles and actuation times. To improve the robot displacement, these variables were improved using random search optimization. The developed actuator is a proposal for soft mechanisms and welcomes the exploration of auxiliary mechanisms and materials in the design of actuators and soft robots. It is worth highlighting that the distance traveled in each step of the robot is not constant since it depends on the environment in which the tests are carried out, that is, the terrain it travels on. It would be interesting to carry out mathematical modeling of the system that allows the application of position and velocity control.

In this article, we opted for a gait optimization process and not for a control process with feedback, since the manufacture of the proposed mechanism was carried out during the first months of confinement due to the health contingency caused by SARS CoV 2, so its manufacture was carried out in the researchers' house with low-end 3D printers. This caused imperfections in manufacturing that made control very difficult. However, some researchers have touched on the subject of imperfect dynamical system control [41], which would be adequate for the control of a system with these manufacturing restrictions, a scheme that we would like to explore in future developments of the proposed mechanism.

Finally, the proposed compliant structure and actuator could be used to design different kinds of legged robots. It is possible to consider several configurations for the actuator to construct different types of mobile soft robots by exchanging both the horizontal or vertical disposition of the limbs or adding more links that the type of robot requires, such as bipedal robot, quadruped robot, and so on.

Data Availability

The data that support the findings of this study are available from the corresponding author, A. Lopez-González (alexandro.lopez@ibero.mx), upon reasonable request.

Conflicts of Interest

The authors declare that they have no conflicts of interest.

Acknowledgments

This research was supported by the Universidad Iberoamericana (Ibero DCI-002847 and Convocatoria 14 DINV) and the Universidad EIA (CO12021002).

References

[1] C. Majidi, "Soft-matter engineering for soft robotics," *Advanced Materials Technologies*, vol. 4, Article ID 1800477, 2018.

[2] K. Suzumori, S. Iikura, and H. Tanaka, "Applying a flexible microactuator to robotic mechanisms," *IEEE Control Systems Magazine*, vol. 12, no. 1, pp. 21–27, 1992.

[3] E. Guizzo, "Soft robotics [turning point]," *IEEE Robotics and Automation Magazine*, vol. 19, no. 1, pp. 128–125, 2012.

[4] D. Trivedi, C. D. Rahn, W. M. Kier, and I. D. Walker, "Soft robotics: biological inspiration, state of the art, and future research," *Applied Bionics and Biomechanics*, vol. 5, no. 3, pp. 99–117, 2008.

[5] M. Bucolo, A. Buscarino, L. Fortuna, and S. Gagliano, "Ebatronics: a new paradigm for experimental laboratory in applied science and technology," *The Physical Educator*, vol. 3, no. 4, 2021.

[6] R. Niiyama, X. Sun, C. Sung, B. An, D. Rus, and S. Kim, "Pouch motors: printable soft actuators integrated with computational design," *Soft Robotics*, vol. 2, no. 2, pp. 59–70, 2015.

[7] M. A. Karimi, V. Alizadehyazdi, B.-P. Busque, H. M. Jaeger, and M. Spenko, "A boundary-constrained swarm robot with granular jamming," in *Proceedings of the 2020 3rd IEEE International Conference on Soft Robotics (RoboSoft)*, IEEE, New Haven, CT, USA, July 2020.

[8] G. Alici, "Softer is harder: what differentiates soft robotics from hard robotics?" *MRS Advances*, vol. 3, no. 28, pp. 1557–1568, 2018.

[9] K. M. Digumarti, A. T. Conn, and J. Rossiter, "Euglenoid-inspired giant shape change for highly deformable soft robots," *IEEE Robotics and Automation Letters*, vol. 2, no. 4, pp. 2302–2307, 2017.

[10] K. Asaka and H. Okuzaki, *Soft Actuators*, Springer, Berlin, Germany, 2014.

[11] D. Rus and M. T. Tolley, "Design, fabrication and control of soft robots," *Nature*, vol. 521, no. 7553, pp. 467–475, 2015.
[12] C. Laschi and M. Cianchetti, "Soft robotics: new perspectives for robot bodyware and control," *Frontiers in Bioengineering and Biotechnology*, vol. 2, p. 3, 2014.
[13] J. Kim, J. W. Kim, H. C. Kim, L. Zhai, H.-U. Ko, and R. M. Muthoka, "Review of soft actuator materials," *International Journal of Precision Engineering and Manufacturing*, vol. 20, no. 12, pp. 2221–2241, 2019.
[14] A. G. Mark, S. Palagi, T. Qiu, and P. Fischer, "Auxetic metamaterial simplifies soft robot design," in *Proceedings of the IEEE International Conference on Robotics and Automation (ICRA)*, IEEE, Stockholm, Sweden, June 2016.
[15] K. E. Evans and A. Alderson, "Auxetic materials: functional materials and structures from lateral thinking!" *Advanced Materials*, vol. 12, no. 9, pp. 617–628, 2000.
[16] L. Gibson, *Cellular Solids: Structure and Properties*, Cambridge University Press, Cambridge, NY, USA, 1997.
[17] T.-C. Lim, *Auxetic Materials and Structures*, Springer, Berlin, Germany, 2015.
[18] P. U. Kelkar, H. S. Kim, K.-H. Cho, J. Y. Kwak, C.-Y. Kang, and H.-C. Song, "Cellular auxetic structures for mechanical metamaterials: a review," *Sensors*, vol. 20, no. 11, p. 3132, 2020.
[19] J. I. Lipton, R. MacCurdy, Z. Manchester, L. Chin, D. Cellucci, and D. Rus, "Handedness in shearing auxetics creates rigid and compliant structures," *Science*, vol. 360, no. 6389, pp. 632–635, 2018.
[20] K. Bertoldi, V. Vitelli, J. Christensen, and M. van Hecke, "Flexible mechanical metamaterials," *Nature Reviews Materials*, vol. 2, no. 11, Article ID 17066, 2017.
[21] A. Sedal, A. H. Memar, T. Liu, Y. Menguc, and N. Corson, "Design of deployable soft robots through plastic deformation of kirigami structures," *IEEE Robotics and Automation Letters*, vol. 5, no. 2, pp. 2272–2279, 2020.
[22] J. Ou, Z. Ma, J. Peters, S. Dai, N. Vlavianos, and H. Ishii, "KinetiX—designing auxetic-inspired deformable material structures," *Computers and Graphics*, vol. 75, pp. 72–81, 2018.
[23] A. Milojević, S. Linß, Ž. Ćojbašić, and H. Handroos, "A novel simple, adaptive, and versatile soft-robotic compliant two-finger gripper with an inherently gentle touch," *Journal of Mechanisms and Robotics*, vol. 13, no. 1, 2021.
[24] Q. Pan, S. Chen, F. Chen, and X. Zhu, "Programmable soft bending actuators with auxetic metamaterials," *Science China Technological Sciences*, vol. 63, no. 12, pp. 2518–2526, 2020.
[25] M. F. Simons, K. M. Digumarti, A. T. Conn, and J. Rossiter, "Tiled auxetic cylinders for soft robots," in *Proceedings of the 2019 2nd IEEE International Conference on Soft Robotics (RoboSoft)*, IEEE, Seoul, Korea, April 2019.
[26] A. Alderson and K. L. Alderson, "Auxetic materials," *Proceedings of the Institution of Mechanical Engineers—Part G: Journal of Aerospace Engineering*, vol. 221, no. 4, pp. 565–575, 2007.
[27] J. N. Grima and K. E. Evans, "Auxetic behavior from rotating squares," *Journal of Materials Science Letters*, vol. 19, no. 17, pp. 1563–1565, 2000.
[28] K. K. Saxena, R. Das, and E. P. Calius, "Three decades of auxetics research—materials with negative poisson's ratio: a review," *Advanced Engineering Materials*, vol. 18, no. 11, pp. 1847–1870, 2016.
[29] J. Angeles, *Rational Kinematics*, Springer-Verlag, New York, NY, USA, 1988.
[30] D. H. Myszka, *Máquinas Y Mecanismos Pearson Educacón*, Pearson, Naucalpan De Juárez, México, 2012.
[31] J. T. Bryson, X. Jin, and S. K. Agrawal, "Optimal design of cable-driven manipulators using particle swarm optimization," *Journal of Mechanisms and Robotics*, vol. 8, no. 4, pp. 0410031–410038, 2016.
[32] H. Banerjee, N. Pusalkar, and H. Ren, "Single-motor controlled tendon-driven peristaltic soft origami robot," *Journal of Mechanisms and Robotics*, vol. 10, no. 6, 2018.
[33] N. Lobontiu, *Compliant Mechanisms: Design of Flexure Hinges*, CRC Press, Boca Raton, FI, USA, 2003.
[34] Y. Tian, B. Shirinzadeh, D. Zhang, and Y. Zhong, "Three flexure hinges for compliant mechanism designs based on dimensionless graph analysis," *Precision Engineering*, vol. 34, no. 1, pp. 92–100, 2010.
[35] D. J. Todd, *Walking Machines: An Introduction to Legged Robots*, Springer US, Boston, MA, USA, 1985.
[36] A. Kandhari, A. Mehringer, H. J. Chiel, R. D. Quinn, and K. A. Daltorio, "Design and actuation of a fabric-based worm-like robot," *Biomimetics*, vol. 4, no. 1, p. 13, 2019.
[37] A. D. Horchler, A. Kandhari, K. A. Daltorio et al., "Worm-like robotic locomotion with a compliant modular mesh," in *Proceedings of the 4th International Conference onBiomimetic and Biohybrid Systems*, pp. 26–37, Springer International Publishing, Berlin, Germany, July 2015.
[38] C. Huang, F. Xie, X.-J. Liu, and Q. Meng, "Measurement configuration optimization and kinematic calibration of a parallel robot," *Journal of Mechanisms and Robotics*, vol. 14, no. 3, 2021.
[39] S. V. Konstantinov, A. I. Diveev, G. I. Balandina, and A. A. Baryshnikov, "Comparative research of random search algorithms and evolutionary algorithms for the optimal control problem of the mobile robot," in *Proceedings of the 13th International Symposium "Intelligent Systems 2018" (INTELS'18)*, St. Petersburg, Russia, October, 2018.
[40] A. Allevato, M. Pryor, and A. L. Thomaz, "Multiparameter real-world system identification using iterative residual tuning," *Journal of Mechanisms and Robotics*, vol. 13, no. 3, 2021.
[41] M. Bucolo, A. Buscarino, C. Famoso, L. Fortuna, and M. Frasca, "Control of imperfect dynamical systems," *Nonlinear Dynamics*, vol. 98, no. 4, pp. 2989–2999, 2019.